 doi:10.20944/preprints202108.0316.v1

Article

Pressure Transient Analysis for Horizontal Wells in Coal Bed Methane Reservoirs with Pressure-Sensitive Permeabilities

Juan Camilo Sepúlveda [1], Sebastián Díaz [2,] * and Edwin Alexander López [3]

[1] Universidad Nacional de Colombia - Sede Medellín, UNAL, Kra 80 No 65-223; jucsepulveda@unal.edu.co
[2] Universidad Nacional de Colombia - Sede Medellín, UNAL, Kra 80 No 65-223; sebdiazgon@unal.edu.co
[3] universidad Nacional de Colombia - Sede Medellín, UNAL, Kra 80 No 65-223; ealopez@unal.edu.co
* Correspondence: sebdiazgon@unal.edu.co

Abstract: Coal bed methane (CBM) reservoirs are complex systems whose properties differ from those of conventional reservoirs. Coal seams are dual-porosity systems that comprise the porosities of the matrix and cleat system. Gas in the coal seams can be stored as free gas in the cleat system and as adsorbed gas in the porous medium. The flow mechanisms of the natural gas through the formation include desorption, diffusion, and Darcy's flow regimes. The permeability of CBM reservoirs is more sensitive to pressure variations than conventional gas reservoirs. To study the flow behavior of CBM reservoirs it is mandatory to use a model that considers their unique characteristics. The objective of this study was to propose a physical and mathematical model of production performance for horizontal wells in CBM reservoirs whose permeability is dependent on pressure. A solution for the model was obtained by applying Pedrosa´s transformation, perturbation theory, Laplace transformation, the point source method, and Sthefest´s algorithm. The solution to this problem was validated with previous work thoroughly. The type curves of the model were built and the pressure transient behavior of the model was analyzed and discussed. The effects of several parameters on pressure behavior were also discussed.

Keywords: Horizontal well, Coal bed methane reservoir, Apparent permeability modulus, Pseudo-steady state diffusion, Pressure transient analysis.

1. Introduction

Coal bed methane (CBM) refers to the natural gas, mainly methane, that is generated and stored in coal seams [1, 2]. Minor amounts of carbon dioxide, nitrogen, hydrogen sulfide, and sulfur dioxide make up the other components of coal bed gas [3]. CBM is an unconventional gas resource that has emerged as an important energy source over the last decades and will play an important role in the future of the energy industry due to the vast amounts of CBM stored in coal seams [1, 3, 4]. Current estimates of total global CBM resources are estimated to be within 113 to 184 Tm^3, of which a total of 42 Tm^3 are recoverable [5, 6].

Because of the enormous amounts of CBM resources available to be recovered, the oil and gas industry has driven a lot of attention to the CBM reservoirs. However, the characteristics of CBM reservoirs differ considerably from those of conventional reservoirs [1, 4]. CBM reservoirs are considered to be dual-porosity systems that comprise the micropores of the matrix and the cleat system [1, 7]. Gas in the coal seams can be stored as free gas in the cleat system and as adsorbed gas in the micropores of the matrix [1, 7]. The flow mechanisms of transport of natural gas through the formation include desorption, diffusion, and Darcy´s flow [1]. For CBM reservoirs the permeability refers to the permeability of the cleats, which act as channels for the seepage process of coal beds [8]. This petrophysical property of CBM reservoirs is more sensitive to the variation of pressure than gas conventional reservoirs. Also, CBM reservoirs are highly heterogeneous formations whose properties and permeabilities depend on aspects such as geological age, coal rank and purity, and sorbed gas content [9].

 doi:10.20944/preprints202108.0316.v1

Due to the characteristics of coal beds, it is necessary to evaluate and determine the properties of CBM reservoirs under dynamic conditions [10]. Well testing is a powerful tool to characterize gas reservoirs (Nie and Ding 2010), and it is the only effective way to evaluate the properties of CBM reservoirs under dynamic conditions [10]. Several authors have studied the pressure transient behavior of horizontal wells in CBM reservoirs. King and Ertekin [11] developed a numerical simulator capable of modeling the performance of vertical fractured or horizontal wells in coal seams. Engler and Rajtar [12] studied the pressure transient responses of a horizontal well in a CBM reservoir, comparing the analytical solution of their model with numerical simulation data. Sarkar and Rajtar [13] developed an analytical solution to study the pressure response of a horizontal well in a CBM reservoir, taking into account the effects of wellbore storage and skin factor. Clarkson et al. [14] used pressure transient analysis to study the behavior of single-phase and multi-phase flow of both hydraulically fractured and horizontal wells in CBM reservoirs. Nie et al. [15] used transient analysis to study the flow behavior of a CBM horizontal well and how it is affected by boundary conditions. Wei et al. (2017) studied the production performance of horizontal wells in composite CBM reservoirs applying transient analysis. Jiang et al. [16] applied transient analysis to study the behavior of multi-branched horizontal wells in stress-sensitive two-regions composite CBM reservoirs. As can be seen from the above literature, many researchers have studied the production performance of horizontal wells in CBM reservoirs, but little is related to coal seams with pressure-sensitive permeabilities. Therefore, the main objective of this article is to study the pressure transient behavior of a horizontal well in a CBM reservoir considering permeability changes by pressure variations, related to production/injection processes.

This work is divided into five sections: first, the physical model is presented. In the second section, the mathematical model is developed. The third section shows the solution of the model developed in the third part. The fourth section presents the results obtained referring to validation and sensitivity analysis of model parameters. Finally, conclusions and references are presented.

2. Physical model

This section is divided into the production scenario, where assumptions and conditions of the model are proposed and after the flow model is described.

2.1. Production scenario

It is considered a cylindrical CBM reservoir that meets the following characteristics:

1. The reservoir is a double-porosity system composed of the porosities of the matrix and cleat system.
2. It is supposed to be laterally infinite.
3. It possesses two closed boundaries, one at the top and the other at bottom of the formation.
4. It has a uniform thickness of h and an initial pressure P_i.
5. A horizontal well is located at the center of the reservoir. The well length is L and it produces at a constant rate (see **Figure 1**).
6. The flux along the horizontal wellbore is supposed to be uniform. This assumption makes it possible to use the point source method.
7. The effects of the wellbore storage and skin factor are considered as well as the effect of the permeability modulus.
8. Isotropic conditions are assumed.

Preprints (www.preprints.org) | NOT PEER-REVIEWED | Posted: 16 August 2021 doi:10.20944/preprints202108.0316.v1

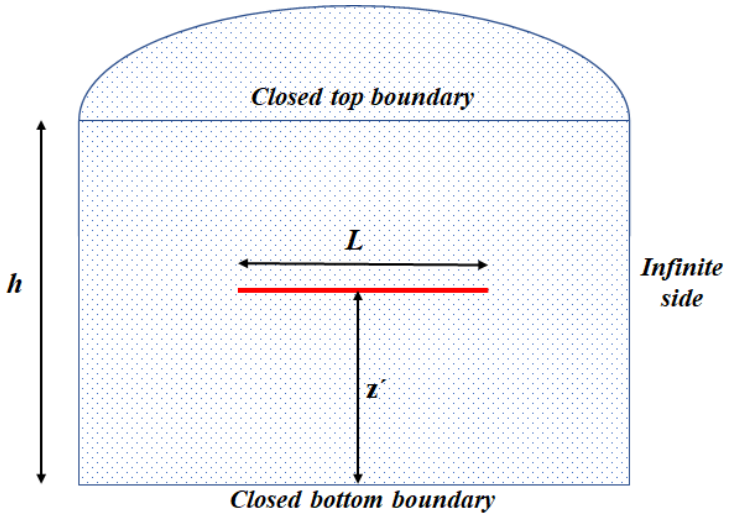

Figure 1. Schematic production scenario used for the mathematical model.

2.2. Flow model

Three flow regimes are considered during the CBM production process (see **Figures 2** and **3**), which are delimitated by the Knudsen coefficient. They are as follows:

1. The gravity, capillary, and viscous forces are neglected.
2. Laminar and isothermal flow is considered.
3. The reservoir is completely saturated with a single phase, and the water in the coal has been completely expelled.

Three flow regimes are considered during the CBM production process (see **Figures 2** and **3**). They are as follows:

- Desorption: where the pressure drop in the cleat system causes the detachment of the gas from the matrix grains. This phenomenon is assumed to be described by the Langmuir model.
- Diffusion: here, the gas is scattered by the concentration gradient and/or mechanical effects through the matrix into the cleats. A pseudo-steady state diffusion is assumed.
- Macroscopic flow in the cleat system: the gas into the cleats obeys Darcy's law and flows into the wellbore due to the pressure drop.

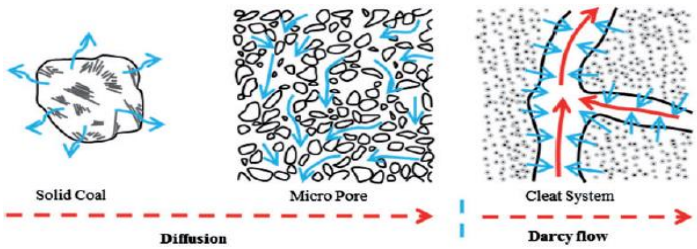

Figure 2. Gas storage and transport in coal seams [17].

Preprints (www.preprints.org) | NOT PEER-REVIEWED | Posted: 16 August 2021 doi:10.20944/preprints202108.0316.v1

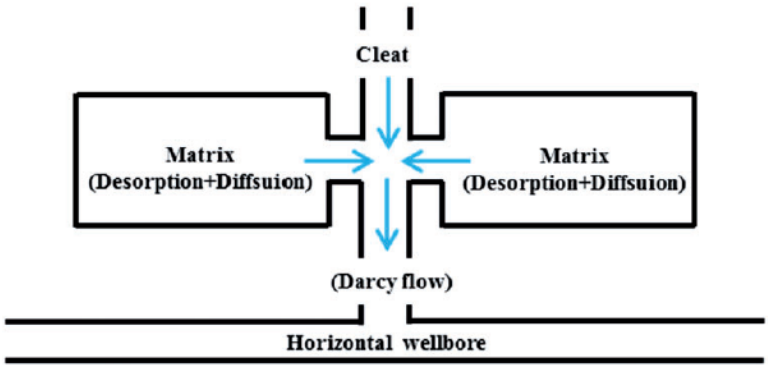

Figure 3. Flow process of CBM in coal seams [17].

3. Theoretical model

This model is composed of mathematical and dimensionless mathematical models. Here are presented important aspects related to the construction of the model.

3.1. Mathematical model

According to considerations of the physical model, the flow equation can be derived by coupling the mass conservation law, the equation state of real gas, Darcy's law, and the pseudo-steady state diffusion equation

$$\frac{1}{r}\frac{\partial}{\partial r}\left(r\frac{P}{Z}\frac{k_h}{\mu}\frac{\partial P}{\partial r}\right)+\frac{1}{r^2}\frac{\partial}{\partial \theta}\left(\frac{P}{Z}\frac{k_h}{\mu}\frac{\partial P}{\partial \theta}\right)+\frac{\partial}{\partial z}\left(\frac{P}{Z}\frac{k_v}{\mu}\frac{\partial P}{\partial z}\right)=\phi C_t\frac{P}{Z}\frac{\partial P}{\partial t}+\frac{P_{sc}T}{T_{sc}}\frac{\partial V_m}{\partial t} \quad (1)$$

The flow equation is highly non-linear. To linearize the gas-flow equation the pseudo-pressure approach [17] and the apparent permeability modulus [18] are defined respectively as

$$\psi=\int_{P_i}^{P}\frac{P}{\mu Z}dP \quad (2)$$

$$\gamma=\frac{1}{k}\frac{dk}{d\psi} \quad (3)$$

Assuming a constant apparent permeability modulus and integrating **Equation 3**, the following expression can be obtained

$$k=k_i exp\left(-\gamma(\psi_i-\psi)\right) \quad (4)$$

Substituting **Equations 2**, **3**, and **4** into **Equation 1**, the flow equation is expressed as

$$\frac{\partial^2\psi}{\partial r^2}+\frac{1}{r}\frac{\partial\psi}{\partial r}+\gamma\left(\frac{\partial\psi}{\partial r}\right)^2+\frac{1}{r^2}\frac{\partial^2\psi}{\partial\theta^2}+\frac{1}{r^2}\gamma\left(\frac{\partial\psi}{\partial\theta}\right)^2+\xi\frac{\partial^2\psi}{\partial z^2}+\xi\gamma\left(\frac{\partial\psi}{\partial z}\right)^2 = \frac{exp(\gamma[\psi_i-\psi])}{k_{hi}}\left[(\phi\mu C_t)\frac{\partial\psi}{\partial t}+\frac{P_{sc}T}{T_{sc}}\frac{\partial V_m}{\partial t}\right] \quad (5)$$

The Langmuir adsorption model is used to characterize the desorption of the gas from matrix grain [19]:

$$V_E=\frac{V_L\psi}{\psi_L+\psi} \quad (6)$$

The diffusion of the gas through the matrix can be described by the pseudo-steady state diffusion model as follows [11, 13]

$$\frac{\partial V_m}{\partial t}=-D\alpha(V_m-V_E) \quad (7)$$

The initial and boundary conditions of the model are defined as

Preprints (www.preprints.org) | NOT PEER-REVIEWED | Posted: 16 August 2021 doi:10.20944/preprints202108.0316.v1

Initial condition

$$\psi = \psi_i, \quad \forall\, r \;\; when \;\; t = 0 \tag{8}$$

Top and bottom conditions

$$\frac{\partial \psi}{\partial z} = 0, \qquad when \;\; z = 0 \;\; or \;\; z = h \tag{9}$$

Outer lateral condition

$$\lim_{r \to \infty} \psi = \psi_i \,, \quad \forall t \tag{10}$$

To describe the point source, the spherical coordinate system is used. Thus, the inner conditions when the point source is in the inner and outer regions, respectively, are defined as

$$\lim_{R \to 0} \frac{T_{sc}}{P_{sc} T} 4\pi \sqrt{\xi} k_{hi} exp(-\gamma[\psi_i - \psi]) R^2 \frac{\partial \psi}{\partial R} = -\tilde{q} \tag{11}$$

3.1. Dimensionless mathematical model

The definitions of the dimensionless variables are presented in **Appendix A**. According to this, **Equation 5** is expressed as

$$\frac{\partial^2 \psi_D}{\partial r_D^2} + \frac{1}{r_D}\frac{\partial \psi_D}{\partial r_D} - \gamma_D \left(\frac{\partial \psi_D}{\partial r_D}\right)^2 + \frac{1}{r_D^2}\frac{\partial^2 \psi_D}{\partial \theta^2} - \frac{1}{r_D^2}\gamma_D \left(\frac{\partial \psi_D}{\partial \theta}\right)^2 + \frac{\partial^2 \psi_D}{\partial z_D^2} - \gamma_D \left(\frac{\partial \psi_D}{\partial z_D}\right)^2 = exp(\gamma_D \psi_D)\left[\omega \frac{\partial \psi_D}{\partial t_D} + (1-\omega)\frac{\partial V_{mD}}{\partial t_D}\right] \tag{12}$$

In **Appendix B,** Pedrosa´s transformation and perturbation transformation are defined. Considering the **Appendix B** and taking into account that the value of γ_D is very small, the zero-order solution is accurate enough to meet precision requirements, and **Equation 12** is simplified as

$$\frac{1}{r_D}\frac{\partial}{\partial r_D}\left(r_D \frac{\partial \eta_0}{\partial r_D}\right) + \frac{1}{r_D^2}\frac{\partial^2 \eta_0}{\partial \theta^2} + \frac{\partial^2 \eta_0}{\partial z_D^2} = \omega \frac{\partial \eta_0}{\partial t_D} + (1-\omega)\frac{\partial V_{mD}}{\partial t_D} \tag{13}$$

Now, writing the storage term variation as a function of the free and adsorbed gas, the following expression is obtained

$$(1-\omega)\frac{\partial V_{mD}}{\partial t_D} = -\lambda(V_{mD} - \beta \eta_0) \tag{14}$$

Applying Laplace transformation to **Equations 13** and **14**, the following equations can be obtained

$$\frac{1}{r_D}\frac{\partial}{\partial r_D}\left(r_D \frac{\partial \bar{\eta}_0}{\partial r_D}\right) + \frac{1}{r_D^2}\frac{\partial^2 \bar{\eta}_0}{\partial \theta^2} + \frac{\partial^2 \bar{\eta}_0}{\partial z_D^2} = u\omega\bar{\eta}_0 + u(1-\omega)\bar{V}_{mD} \tag{15}$$

$$u(1-\omega)\bar{V}_{mD} = -\lambda(\bar{V}_{mD} - \beta\bar{\eta}_0) \tag{16}$$

Substituting **Equation 16** into **Equation 15**, the dimensionless flow equation can be expressed as

$$\frac{1}{r_D}\frac{\partial}{\partial r_D}\left(r_D \frac{\partial \bar{\eta}_0}{\partial r_D}\right) + \frac{1}{r_D^2}\frac{\partial^2 \bar{\eta}_0}{\partial \theta^2} + \frac{\partial^2 \bar{\eta}_0}{\partial z_D^2} = f(u)\bar{\eta}_0 \tag{17}$$

Where $f(u)$ is given by

$$f(u) = u\omega + u(1-\omega)\left(\frac{\lambda\beta}{u(1-\omega)+\lambda}\right) \tag{18}$$

Preprints (www.preprints.org) | NOT PEER-REVIEWED | Posted: 16 August 2021 doi:10.20944/preprints202108.0316.v1

Applying the definition of dimensionless variables, Pedrosa´s transformation, and perturbation transformation [18], the boundary conditions of the model, expressed by **Equations 8** through **11**, become in

$$\bar{\eta}_0 = 0, \quad \forall\, r_D \;\; when \;\; u \to \infty \tag{19}$$

$$\frac{\partial \bar{\eta}_0}{\partial z_D} = 0, \qquad when \;\; z_D = 0 \;\; or \;\; z_D = h_D \tag{20}$$

$$\lim_{r_D \to \infty} \bar{\eta}_0 = 0\,, \quad \forall\, u \tag{21}$$

$$\lim_{R \to 0} 2\sqrt{\xi}\frac{L}{h} R_D^2 \frac{\partial \bar{\eta}_0}{\partial R_D} = \frac{\tilde{q}_D}{u} \tag{22}$$

4. Solution of the model

To solve the model the point source method is applied. The detailed derivation is presented in **Appendix C**. By integrating the point source pressure distribution regarding r'_D from -1 to 1, the pressure distribution for the horizontal well is

$$\bar{\eta}_{HDN} = \int_{-1}^{1} \bar{\eta}_{DN1}|_{\theta'=0} dr'_D \tag{23}$$

To obtain the pressure distribution through the reservoir the integral average method is applied

$$\bar{\eta}_{WD} = \frac{1}{2}\int_{-1}^{1} \bar{\eta}_{HDN}|_{\theta=0} dr_D \tag{24}$$

Applying Duhamel's principle [20], the solution of the flow equation considering the effects of wellbore storage and skin factor can be obtained as

$$\bar{\eta}_{WD}(C_D, S) = \frac{u\bar{\eta}_{WD} + S}{u + C_D u^2 (u\bar{\eta}_{WD} + S)} \tag{25}$$

Stehfest´s numerical inversion method [21] and Pedrosa´s transformation [18] can be used to obtain the pressure response of the reservoir in the real-time domain

$$\psi_{WD}(C_D, S) = -\frac{1}{\gamma_D} Ln(1 - \gamma_D L\{\bar{\eta}_{WD}(C_D, S)\}^{-1}) \tag{26}$$

5. Results

In this section, results are presented and analyzed. First, the validation of the model is described, after the type curve characteristics of CBM reservoirs are showed, then sensitivities of several parameters are made.

5.1. Validation of the model

To study CBM reservoirs with pressure-sensitive permeabilities, flow and formation parameters proposed in previous models were included, which describe the flow dynamics also present in CBM reservoirs. Therefore, the model proposed in this article, under specific conditions, must be able to emulate the behavior of other types of reservoirs, described by simpler models. In **Figure 4** can be seen that the type curves generated matched the Bourdet and Gringarten chart, which indicates that this proposed model is reliable.

Preprints (www.preprints.org) | NOT PEER-REVIEWED | Posted: 16 August 2021 doi:10.20944/preprints202108.0316.v1

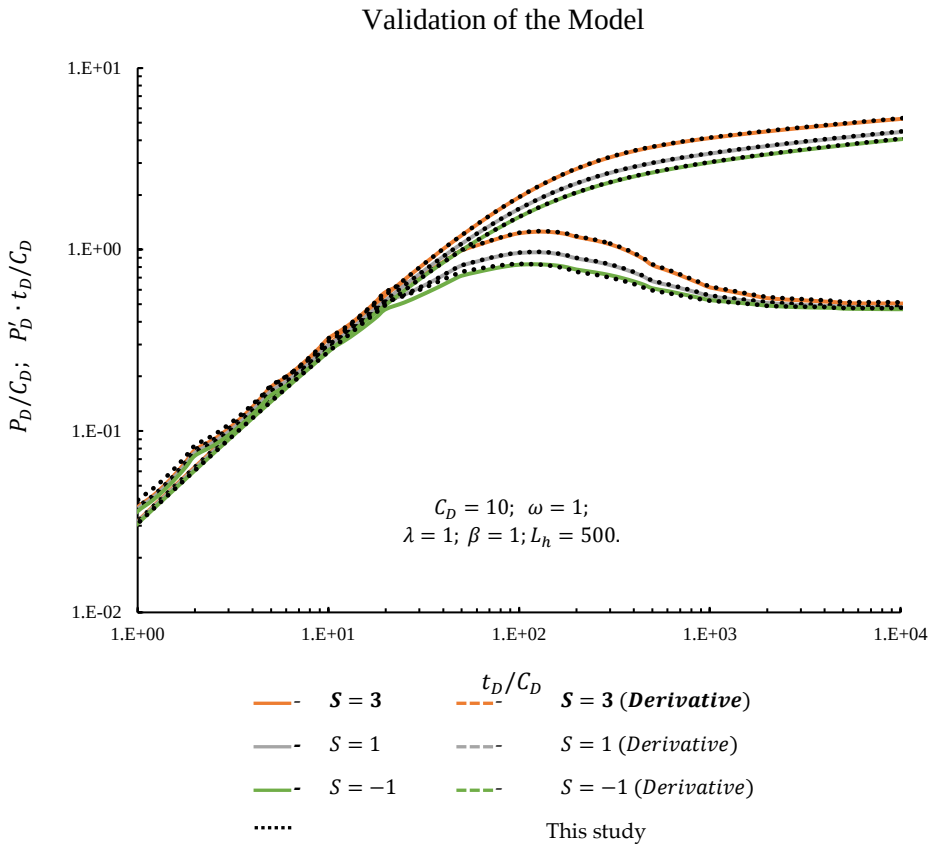

Figure 4. Validation of the Model**.**

5.2. Type curves of horizontal wells in CBM reservoirs with pressure-sensitive permeabilities

Figure 5 illustrates the type curves for dimensionless wellbore pressure (P_D/C_D) and dimensionless wellbore pressure derivative $(P'_D \cdot t_D/C_D)$ concerning dimensionless time (t_D/C_D).

Regime I: The wellbore storage period. The slope is unitary in both pressure and pressure derivative curves.

Regime II: The skin factor period. Here the pressure perturbation goes through the skin near to the wellbore. Regime II is characterized by a hump in the pressure derivative curve due to the additional pressure drop in the skin zone.

Regime III: The radial flow period. Typically, the value of the dimensionless pressure derivative in the radial flow regime is 0.5. However, in **Figure 5** the value of the dimensionless pressure derivative in this flow regime is around 0.57 due to the effect of the dimensionless apparent permeability modulus that causes a higher pressure drop to keep constant the flow rate.

Regime IV: Transition regime. In this period, the gas flows from the matrix toward fractures because the pressure in cleats decreases and gas desorption and diffusion become an important supplement. This flow regime is typical of dual-porosity systems.

Regime V: Late pseudo-radial flow regime. This flow period occurs when the gas flow from matrix to cleats reaches a dynamic equilibrium with the flow from cleats to the wellbore. The value dimensionless pressure and dimensionless derivative increase due to the effect dimensionless apparent permeability modulus.

Preprints (www.preprints.org) | NOT PEER-REVIEWED | Posted: 16 August 2021 doi:10.20944/preprints202108.0316.v1

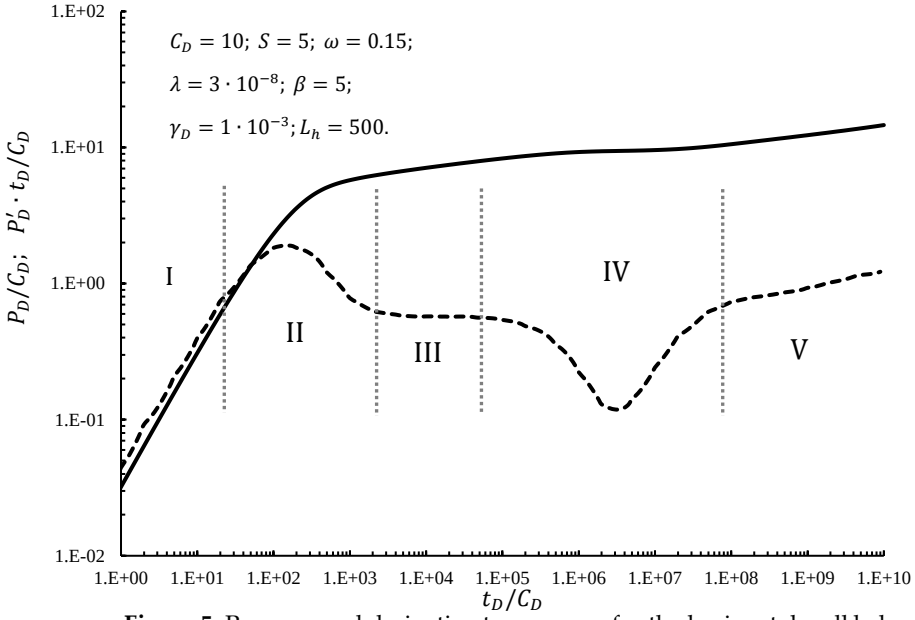

Figure 5. Pressure and derivative type curves for the horizontal well behavior.

It is noticed that there are not present in **Figure 5** a transition regime that should appear after Regime III, and a second radial flow regime that should appear after the transition regime and before Regime IV. This occurs due to uncertainties of the computational model which still must be refined to capture the complete flow behavior of the reservoir. Transition and second radial flow regimes are typical of horizontal wells.

5.3. Sensitivity analysis

This section presents results obtained from parametric variations such as skin factor, storage capacity coefficient, interporosity flow coefficient, and dimensionless apparent permeability modulus.

5.3.1. Effect of the skin factor

Figure 6 shows the behavior of the type curves with the variation of the skin factor. Variations of the skin factor between values of -1 and 3 were made. It is observed that as the skin factor increases the pressure drop in the Regime II increases and Regime III is delayed. When producing with a higher skin factor there is higher flow resistance in the skin zone. As result, pressure disturbance spreads more slowly through the skin zone and the pressure drop in this zone is higher to keep constant the production rate.

Preprints (www.preprints.org) | NOT PEER-REVIEWED | Posted: 16 August 2021 doi:10.20944/preprints202108.0316.v1

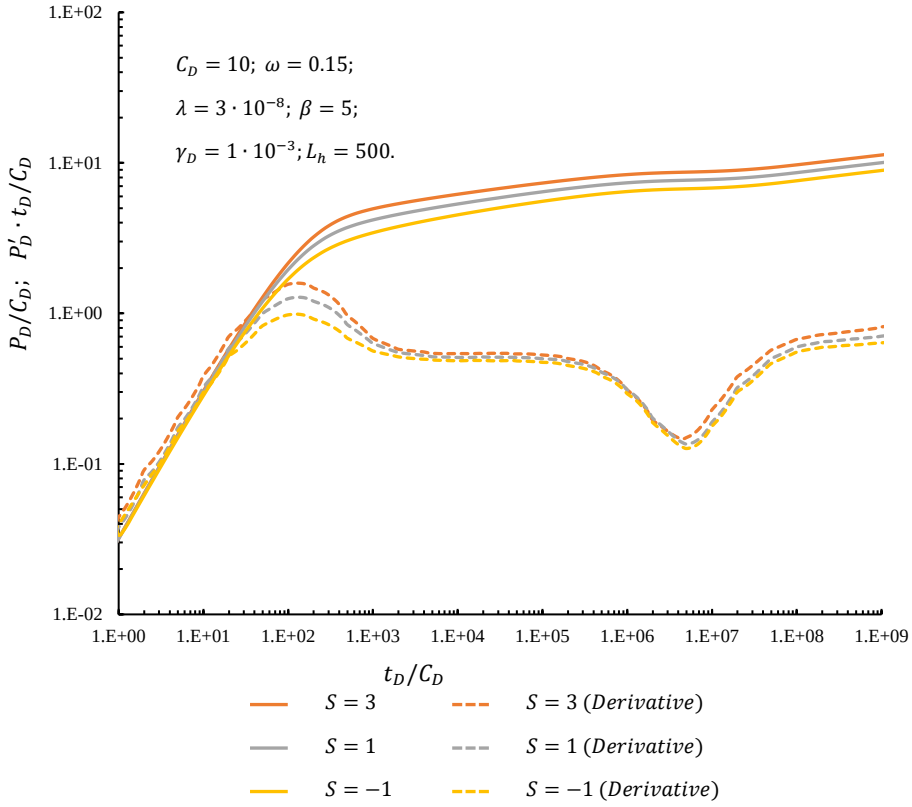

Figure 6. Dimensionless pressure and derivative versus dimensionless time affected by skin factor variations.

5.3.2. Effect of the storage capacity coefficient

Figure 7 presents the effect of the storage capacity coefficient on the type curves. The storage capacity coefficient is varied between 0.1 and 0.3. As can be seen, this coefficient mainly affects the transition regime period. A lower value of this parameter indicates few gas reserves in the cleats. As result, the fractures will be depleted enough to allow the flow from the matrix at earlier times. This leads to an earlier appearance of the transition regime period. Also, a lower storage capacity coefficient causes a deeper "V" shape concave in the same flow period. This occurred because a lower coefficient indicates that reserves in the matrix are larger concerning the reserves in the fractures, and hence the amount of gas flowing from the matrix to the fractures is higher leading to a higher-pressure recovery in the fractures.

Preprints (www.preprints.org) | NOT PEER-REVIEWED | Posted: 16 August 2021 doi:10.20944/preprints202108.0316.v1

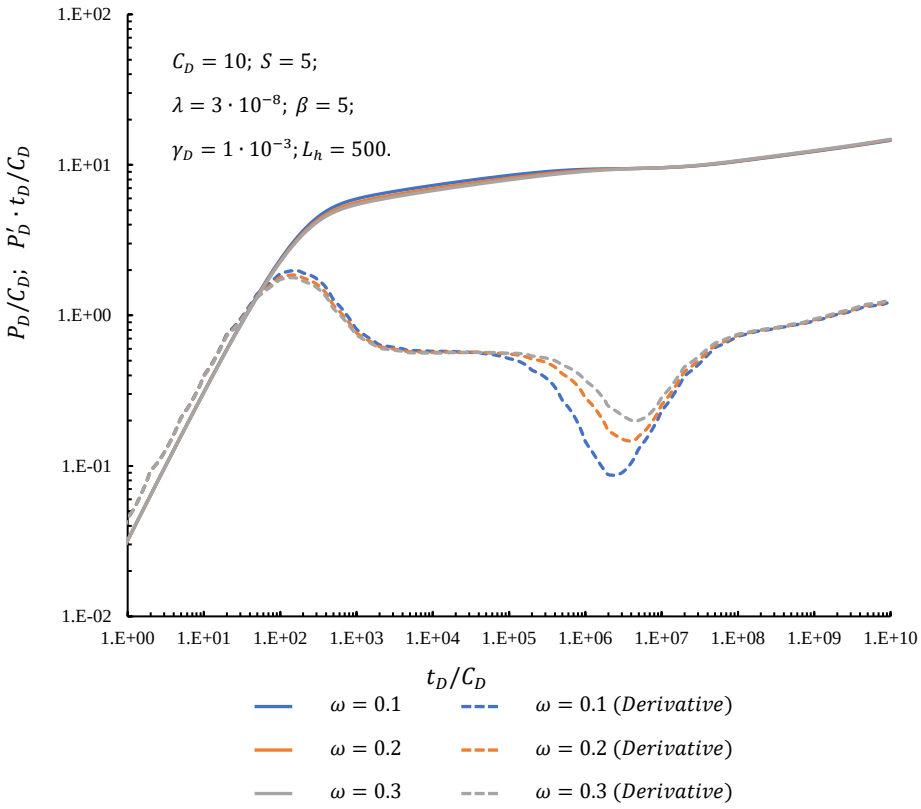

Figure 7. The effect of the storage capacity coefficient on pressure and derivative type curves.

5.3.3. Effect of the interporosity flow coefficient

Figure 8 shows the effects of the interporosity flow coefficient that is varied between 3×10^{-9} and 3×10^{-7}. Interporosity flow coefficient mainly affects Regimes III to V. A smaller interporosity flow coefficient indicates a higher resistance for gas to flow from the matrix to the fractures. As consequence, the duration of the radial flow regime is increased and the appearance of the transition and late pseudo-radial flow regimes is delayed. Also, it is observed that reducing the coefficients reduces as well the deepness of the "V" shape of the transition regime. This is because reducing the coefficient reduces the ability of the gas flowing from the matrix to restore the pressure in the fractures.

Preprints (www.preprints.org) | NOT PEER-REVIEWED | Posted: 16 August 2021 doi:10.20944/preprints202108.0316.v1

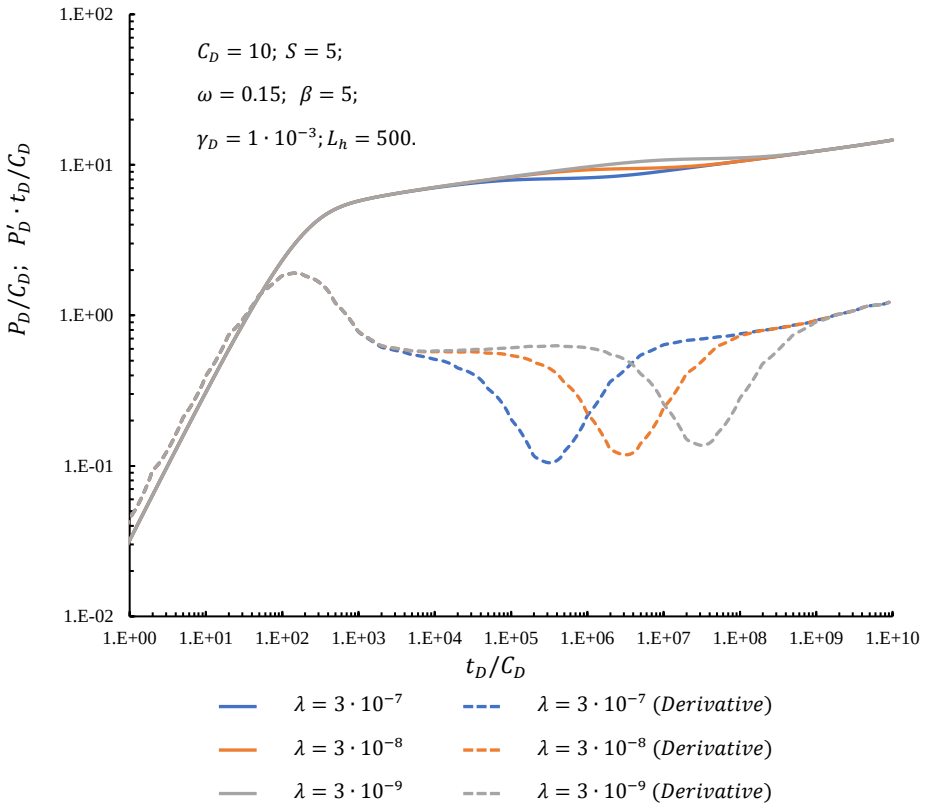

Figure 8. The effect of the interporosity flow coefficient on pressure and derivative type curves.

5.4.4. Effect of the adsorption coefficient

The effect of the adsorption coefficient over both pressure and derivative types curves is observed in **Figure 9**. As shown in **Figure 9**, the adsorption coefficient is varied between 3 and 15. This coefficient mainly affects Regimes III to V. Reducing the adsorption coefficient increases the duration of the radial flow regime and leads to a later appearance of the transition regime as well as makes that the "V" shape be shallower. This behavior occurred because the less the coefficient the less the quantity of gas adsorbed in the matrix. As result, the amount of gas that desorbs from the matrix is lower, increasing the amount of time necessary to reach a high enough pressure in the matrix to obligate the desorbed gas to flow to the fractures.

Preprints (www.preprints.org) | NOT PEER-REVIEWED | Posted: 16 August 2021 doi:10.20944/preprints202108.0316.v1

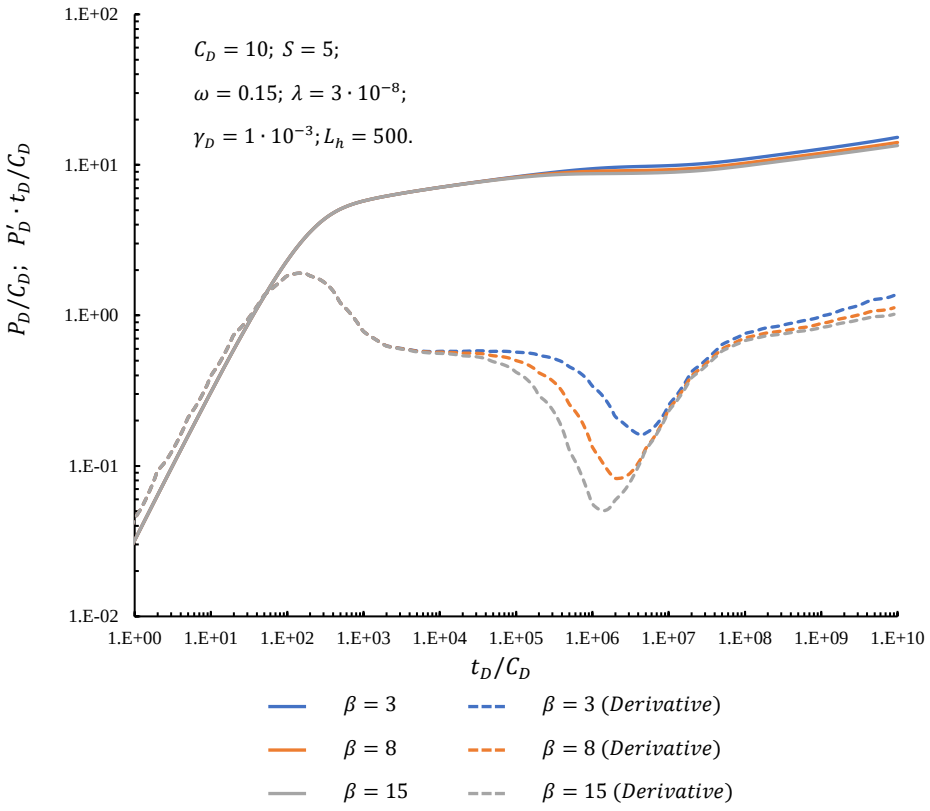

Figure 9. The effect of the adsorption coefficient on pressure and derivative type curves.

5.3.5. Effect of the dimensionless apparent permeability modulus

Figure 10 shows the effect of the dimensionless apparent permeability modulus on pressure and derivative type curves. This parameter is varied between 0 (non-pressure sensitive permeability case) and 0.01. It is noticed that a change in the dimensionless apparent permeability modulus affects all the flow periods except the wellbore storage period. This is because the pressure response associated with different permeability modulus is related to the reservoir. According to **Figure 10**, increasing the modulus increases the pressure drop and slopes of the radial flow and late pseudo-radial flow regimes. This behavior occurred because the more the dimensionless apparent permeability modulus the more the reduction of the permeability due to the pressure changes. Therefore, to keep constant the production rate the pressure drop and rate of change of the pressure drop have to be higher.

Preprints (www.preprints.org) | NOT PEER-REVIEWED | Posted: 16 August 2021 doi:10.20944/preprints202108.0316.v1

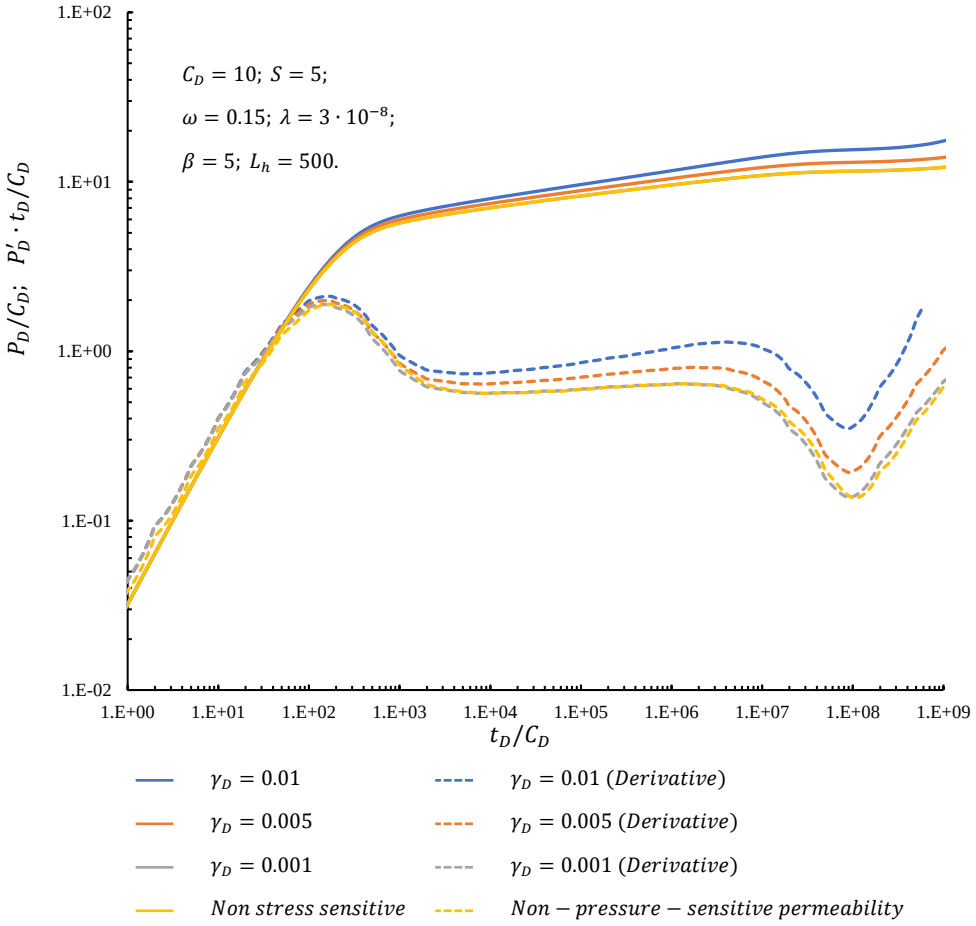

Figure 10. The effect of the dimensionless apparent permeability modulus on pressure and derivative type curves.

6. Discussion

A mathematical model has been developed to describe the pressure behavior of horizontal wells in CBM reservoirs under pressure-sensitive permeabilities and validations have been achieved. According to the results, five flow regimes were identified which depend on the parameters of the model. These regimes are very important because they indicate how the pressure on the wellbore behaves as the pressure disturbance spreads through the reservoir. However, it is noticed that there are not present two flow regimes that should be between Regimes III and IV. The disappeared regimes correspond to the transition regime and second radial flow regime. The transition regime is characterized because during this period the derivative type curve behaves like a straight-line of unitary slope due to the interference of the top and bottom closed barriers. The second radial flow regime is characterized because in this period the derivative type curve behaves like a horizontal whose slope depends on the dimensionless apparent permeability modulus. This is very important because these flow regimes are typical of the behavior of horizontal wells and the effects of the variation of the parameters of the model on these flow regimes should be studied too. The absence of these flow regimes is attributed to uncertainties of the computer model, which must be refined to capture completely the behavior of the horizontal well in the proposed model.

The ω, β, and λ parameters play a significant role in the behavior of the system because they determine the impact of the matrix and the fractures on the pressure response. These parameters mainly affect the Regime IV, which corresponds to the transition regime period, which is particularly important for CBM reservoirs considering that a large amount of the gas stored in the matrix is adsorbed on the grains of the coalbed. Also, ω, β, and λ parameters can affect the duration of the Regimes III and V. The γ_D parameter

 doi:10.20944/preprints202108.0316.v1

is also very relevant because it depends on how much the pressure affects the permeability of the system and vice-versa. Correct determination of γ_D parameter is important to estimate the changes of permeability due to pressure variations, which is necessary to plan the development of the reservoir, especially when the reservoir has been significantly depleted and permeability has decreased importantly which may affect productivity or injection processes. Another important parameter is the skin factor S because it gives an idea about how damaged is the skin zone, however, this parameter is mainly restricted to Regimes II and III.

The major contribution of this paper is related to the coupling of the CBM model with the pressure sensitivity of the permeability by the inclusion of the dimensionless apparent permeability modulus. The sensitivity of the permeability can impact significantly the pressure behavior of the system. However, it is necessary to keep refining the model and extend it for the study of more complex systems such as composite reservoirs, which are characterized by the presence of two regions, one close to the wellbore and another away from it, whose properties vary from each other. Analysis of this kind of model can be achieved by establishing flow equations for each region and applying the point source method to obtain the pressure response, as stated in **Appendix C**.

7. Conclusions

A coupled mathematical model to describe the behavior of transient pressure in CBM reservoirs has been presented and validated. The mathematical model was developed by considering a horizontal well in a CBM reservoir that is naturally fractured and laterally infinite as well as transport mechanisms of gas in the coal matrix and cleats. According to the results presented, the following conclusions were obtained:

- Five flow regimes including the wellbore storage period, skin factor period, radial flow regime, transition regime, and pseudo-late radial regime were identified from the type curves of the reservoir. However, the computational model utilized to build the type curves of this model still must be refined to capture completely the flow behavior of horizontal wells in CBM reservoirs.
- Several parameters including skin factor, interporosity flow coefficient, storage capacity coefficient, adsorption coefficient, and dimensionless apparent permeability modulus were sensitized showing a significant impact on the pressure transient behavior. Also, their effects were analyzed.
- The most relevant contribution of this work is related to the coupling of the CBM model with the pressure sensitivity of the permeability by varying the dimensionless apparent permeability modulus. It is stated that by increasing the dimensionless apparent permeability modulus, both the pressure drop and the rate of change of the pressure drop increase too to keep constant the production rate.

Author Contributions: Conceptualization, Edwin Alexander López; methodology, Sebastián Díaz and Edwin Alexander López; software, Juan Camilo Sepúlveda; validation, Juan Camilo Sepúlveda, Sebastián Díaz, and Edwin Alexander López; formal analysis, Juan Camilo Sepúlveda, Sebastián Díaz, and Edwin Alexander López; data curation, Juan Camilo Sepúlveda and Edwin Alexander López; writing-original draft preparation, Juan Camilo Sepúlveda, Sebastián Díaz, and Edwin Alexander López; writing-review and editing, Juan Camilo Sepúlveda, Sebastián Díaz, Edwin Alexander López; visualization, Juan Camilo Sepúlveda, Sebastián Díaz, and Edwin Alexander López; supervision, Juan Camilo Sepúlveda, Sebastián Díaz, and Edwin Alexander López; project administration, Juan Camilo Sepúlveda, Sebastián Díaz, and Edwin Alexander López.

All authors have read and agreed to the published version of the manuscript.

Funding: This research received no external funding

Acknowledgments: The authors appreciate the support of the National University of Colombia - Medellín Campus, UNAL, during the development of this work.

Conflicts of Interest: The authors declare no conflict of interest.

Appendix A

Preprints (www.preprints.org) | NOT PEER-REVIEWED | Posted: 16 August 2021 doi:10.20944/preprints202108.0316.v1

$$\psi_D = \frac{2\pi k_{hi} h}{q} \frac{T_{sc}}{P_{sc} T} (\psi_i - \psi) \tag{A1}$$

$$r_D = \frac{r}{L} \tag{A2}$$

$$\tilde{q}_D = \frac{\tilde{q}}{q} \tag{A3}$$

$$z_D = \frac{z}{L} \frac{1}{\sqrt{\xi}} \tag{A4}$$

$$\xi = \left(\frac{k_v}{k_h}\right)_i \tag{A5}$$

$$t_D = \frac{t k_{hi}}{L^2} \left(\phi \mu C_t + \frac{2\pi k_{hi} h V_{Ei}}{q}\right)^{-1} \tag{A6}$$

$$\gamma_D = \frac{q}{2\pi k_{hi} h} \frac{P_{sc} T}{T_{sc}} \gamma \tag{A7}$$

$$V_{mD} = \frac{V_{Ei} - V_m}{V_{Ei}} \tag{A8}$$

$$\omega = \frac{(\phi \mu C_t)}{(\phi \mu C_t) + \left(\frac{2\pi k_{hi} h V_{Ei}}{q}\right)} \tag{A9}$$

$$\beta = \left(\frac{\gamma_D}{1 - exp\,(-\gamma_D \psi_D)}\right) \left(\frac{\psi_L (\psi_i - \psi)}{\psi_i (\psi_L + \psi)}\right) \tag{A10}$$

$$\lambda = \frac{2\pi L^2 h D_i \alpha V_{Ei}}{q} \tag{A11}$$

Appendix B

For the sake of the convenience to analytically solve the model, Pedrosa´s transformation is applied [18]

$$\psi_D = -\frac{1}{\gamma_D} Ln(1 - \gamma_D \eta) \tag{B1}$$

Substituting **Equation B1** into **Equation 12** the following equation is obtained

$$\begin{aligned} &\frac{\partial}{\partial r_D}\left(\frac{1}{1-\gamma_D\eta}\frac{\partial \eta}{\partial r_D}\right) + \frac{1}{r_D}\left(\frac{1}{1-\gamma_D\eta}\right)\frac{\partial \eta}{\partial r_D} - \gamma_D\left(\frac{1}{1-\gamma_D\eta}\right)^2\left(\frac{\partial \eta}{\partial r_D}\right)^2 + \\ &\frac{1}{r_D^2}\left(\frac{1}{1-\gamma_D\eta}\right)\frac{\partial^2 \eta}{\partial \theta^2} - \frac{1}{r_D^2}\gamma_D\left(\frac{1}{1-\gamma_D\eta}\right)^2\left(\frac{\partial \eta}{\partial \theta}\right)^2 + \left(\frac{1}{1-\gamma_D\eta}\right)\frac{\partial^2 \eta}{\partial z_D^2} - \\ &\gamma_D\left(\frac{1}{1-\gamma_D\eta}\right)^2\left(\frac{\partial \eta}{\partial z_D^2}\right)^2 = \left(\frac{1}{1-\gamma_D\eta}\right)\left[\omega\left(\frac{1}{1-\gamma_D\eta}\right)\frac{\partial \eta}{\partial t_D} + (1-\omega)\frac{\partial V_{mD}}{\partial t_D}\right] \end{aligned} \tag{B2}$$

Supposing small values of $(\partial\eta/r_D)^2$, $(\partial\eta/\partial\theta)^2$, and $(\partial\eta/\partial z_D)^2$, **Equation B2** can be simplified as

$$\frac{\partial^2 \eta}{\partial r_D^2} + \frac{1}{r_D}\frac{\partial \eta}{\partial r_D} + \frac{1}{r_D^2}\frac{\partial^2 \eta}{\partial \theta^2} + \frac{\partial^2 \eta}{\partial z_D^2} = \omega\left(\frac{1}{1-\gamma_D\eta}\right)\frac{\partial \eta}{\partial t_D} + (1-\omega)\frac{\partial V_{mD}}{\partial t_D} \tag{B3}$$

Preprints (www.preprints.org) | NOT PEER-REVIEWED | Posted: 16 August 2021 doi:10.20944/preprints202108.0316.v1

An approximate analytical solution can be obtained for **Equation B3** applying the perturbation transformation defined as [18]

$$\eta = \eta_0 + \gamma_D\eta_1 + \gamma_D^2\eta_2 + \cdots = \sum_{j=0}^{+\infty}\gamma_D^j\eta_j \tag{B4}$$

$$\frac{1}{1-\gamma_D\eta} = 1 + \gamma_D\eta + \gamma_D^2\eta^2 + \cdots = \sum_{j=0}^{+\infty}\gamma_D^j\eta^j \tag{B5}$$

Substituting **Equations B4** and **B5** into **Equation B3** the following equation can be obtained

$$\frac{\partial^2}{\partial r_D^2}\left(\sum_{j=0}^{+\infty}\gamma_D^j\eta_j\right) + \frac{1}{r_D}\frac{\partial}{\partial r_D}\left(\sum_{j=0}^{+\infty}\gamma_D^j\eta_j\right) + \frac{1}{r_D^2}\frac{\partial^2}{\partial\theta^2}\left(\sum_{j=0}^{+\infty}\gamma_D^j\eta_j\right) + \frac{\partial^2}{\partial z_{1D}^2}\left(\sum_{j=0}^{+\infty}\gamma_D^j\eta_j\right) = \omega\left(\sum_{j=0}^{+\infty}\gamma_D^j\eta^j\right)\frac{\partial}{\partial t_D}\left(\sum_{j=0}^{+\infty}\gamma_D^j\eta_j\right) + (1-\omega)\frac{\partial V_{mD}}{\partial t_D} \tag{B6}$$

Appendix C

The point source method is used to solve the model [17, 22]. The solution proposed by Ozkan [22] allows obtaining the pressure distribution in composite reservoirs that comprise an inner region and an outer region whose properties differ. The pressure distributions for the inner and the outer regions respectively are

$$\begin{aligned}\bar{\eta}_{DN1} &= \frac{1}{2\pi h_{1D}}\left\{\sum_{k=-\infty}^{+\infty}\left[I_k\left(r'_D\sqrt{f_1(u)}\right)K_k\left(r_D\sqrt{f_1(u)}\right)cos\left(k[\theta-\theta']\right)\right]\right. \\ &+ 2\sum_{N=1}^{+\infty}\left[cos\left(N\pi\frac{z_{1D}}{h_{1D}}\right)cos\left(N\pi\frac{z'_{1D}}{h_{1D}}\right)\sum_{k=-\infty}^{+\infty}\left(I_k(r'_D\varepsilon_{N1})K_k(r_D\varepsilon_{N1})cos\left(k[\theta\right.\right.\right. \\ &\left.\left.\left.-\theta']\right)\right)\right] + \sum_{k=-\infty}^{+\infty}\left[c_{k0}I_k\left(r_D\sqrt{f_1(u)}cos\left(k[\theta-\theta']\right)\right)\right] \\ &\left. + 2\sum_{N=1}^{+\infty}\left[cos\left(N\pi\frac{z_{1D}}{h_{1D}}\right)cos\left(N\pi\frac{z'_{1D}}{h_{1D}}\right)\sum_{k=-\infty}^{+\infty}\left(c_{kN}I_k(\varepsilon_{N1}r_D)cos\left(k[\theta-\theta']\right)\right)\right]\right\}\end{aligned} \tag{C1}$$

$$\begin{aligned}\bar{\eta}_{DN2} = \frac{1}{2\pi h_{2D}}&\left\{\sum_{k=-\infty}^{+\infty}\left[d_{k0}K_k\left(r_D\sqrt{f_2(u)}\right)cos\,cos\left(k[\theta-\theta']\right)\right]\right. \\ &+ 2\sum_{N=1}^{+\infty}\left[cos\left(N\pi\frac{z_{2D}}{h_{2D}}\right)cos\left(N\pi\frac{z'_{2D}}{h_{2D}}\right)\sum_{k=-\infty}^{+\infty}\left(d_{kN}K_k(r_D\varepsilon_{N2})cos\left(k[\theta\right.\right.\right. \\ &\left.\left.\left.\left.-\theta']\right)\right)\right]\right\}\end{aligned} \tag{C2}$$

Where

$$\varepsilon_{N1} = \sqrt{f_1(u) + \frac{N^2\pi^2}{h_{1D}^2}} \tag{C3}$$

Preprints (www.preprints.org) | NOT PEER-REVIEWED | Posted: 16 August 2021 doi:10.20944/preprints202108.0316.v1

$$\varepsilon_{N2} = \sqrt{f_2(u) + \frac{N^2\pi^2}{h_{2D}^2}} \tag{C4}$$

According to Ozkan [22] the coefficients c_{kN}, C_{kN}, d_{kN}, and D_{kN} can be obtained by coupling the pressure distributions $\bar{\eta}_{DN1}$and $\bar{\eta}_{DN2}$ with the boundary conditions at the interface between the two regions of the reservoir. For the sake of convenience to solve the model analytically and apply the solution proposed by Ozkan [22], it is assumed that M is equal to 1, h_{1D} is equal to h_{2D}, and $f_2(u)$ is equal to $f_1(u)$, and hence the following expressions can be obtained

$$c_{kN} = -C_{kN} I_k(r'_D \varepsilon_{N1}) \tag{C5}$$

$$C_{kN} = \frac{M\varepsilon_{N1} K'_k(\varepsilon_{N1} r_{1D}) K_k(\varepsilon_{N2} r_{1D}) - \varepsilon_{N2} K'_k(\varepsilon_{N2} r_{1D}) K_k(\varepsilon_{N1} r_{1D})}{M\varepsilon_{N1} I'_k(\varepsilon_{N1} r_{1D}) K_k(\varepsilon_{N2} r_{1D}) - \varepsilon_{N2} I_k(\varepsilon_{N1} r_{1D}) K'_k(\varepsilon_{N2} r_{1D})} \tag{C6}$$

$$d_{kN} = \frac{h_{2D}}{h_{1D}} \frac{M}{r_{1D}} D_{kN} I_k(\varepsilon_{N1} r'_D) \tag{C7}$$

$$D_{kN} = \frac{1}{M\varepsilon_{N1} I'_k(\varepsilon_{N1} r_{1D}) K_k(\varepsilon_{N2} r_{1D}) - \varepsilon_{N2} I_k(\varepsilon_{N1} r_{1D}) K'_k(\varepsilon_{N2} r_{1D})} \tag{C8}$$

Nomenclature

Notation	
C	Wellbore storage factor, m³/Pa
C_t	Total compressibility, Pa⁻¹
D	Diffusion coefficient, m²/s
h	Reservoir thickness, m
$I_k(x)$	The modified Bessel function of first kind
k	Permeability, m²
$K_k(x)$	The modified Bessel function of second kind
L	Length of the horizontal well, m
P	Pressure, Pa
q	Well production rate m³/s
$\tilde{q}$	Point source production rate, m³/s
r, θ, z	Cylindrical coordinates
S	Skin factor, dimensionless
t	Time, s
T	Temperature, K
x, y, z	Cartesian coordinates
u	Variable of Laplace space concerning t_D
V_E	Equilibrium volumetric gas concentration, m³/m³
V_L	Langmuir volume m³/m³
V_m	Volumetric gas concentration, m³/m³
Z	Compressibility factor, fraction
α	Shape factor, m⁻²
β	Adsorption coefficient for matrix, dimensionless
γ	Apparent permeability modulus, Pa⁻¹

η	Variable of Pedrosa´s transformation related to ψ_D
λ	Transfer coefficient, dimensionless
μ	Viscosity, Pa·s
ξ	Vertical permeability to horizontal permeability ratio, fraction
ϕ	Porosity, fraction
ψ	Pseudo-pressure Pa/s
ψ_L	Langmuir pseudo-pressure Pa/s
ω	Storage coefficient, dimensionless

Subscripts and superscripts

D	Dimensionless
i	Initial
h	Horizontal direction
sc	Standard conditions
v	Vertical direction
$^-$	Laplace transformation
0	Zero-order function

References

1. Satter, A. and G.M. Iqbal, *Reservoir engineering: the fundamentals, simulation, and management of conventional and unconventional recoveries*. 2015: Gulf Professional Publishing.
2. Thakur, P., *Advanced reservoir and production engineering for coal bed methane*. 2016: Gulf Professional Publishing.
3. Flores, R.M., *Coalbed methane: from hazard to resource.* International Journal of Coal Geology, 1998. **35**(1-4): p. 3-26.
4. Moore, T.A., *Coalbed methane: a review.* International Journal of Coal Geology, 2012. **101**: p. 36-81.
5. Al-Jubori, A., et al., *Coalbed methane: clean energy for the world.* Oilfield Review, 2009. **21**(2): p. 4-13.
6. Thomas, L., *Coal geology*. 2013: Wiley Online Library.
7. Thakur, P., S.J. Schatzel, and K. Aminian, *Coal bed methane: From prospect to pipeline*. 2014: Elsevier.
8. Yang, Y., X. Peng, and X. Liu, *The stress sensitivity of coal bed methane wells and impact on production.* Procedia Engineering, 2012. **31**: p. 571-579.
9. Kumar, H., M. Mishra, and S. Mishra, *Laboratory investigation of gas permeability and its impact on CBM potential.* Journal of Petroleum Exploration and Production Technology, 2018. **8**(4): p. 1183-1197.
10. Zhuang, H., et al., *Dynamic well testing in petroleum exploration and development*. 2020: Elsevier.
11. King, G.R. and T. Ertekin, *Comparative evaluation of vertical and horizontal drainage wells for the degasification of coal seams.* SPE Reservoir Engineering, 1988. **3**(02): p. 720-734.
12. Engler, T. and J. Rajtar. *Pressure transient testing of horizontal wells in coalbed reservoirs*. in *SPE rocky mountain regional meeting*. 1992. Society of Petroleum Engineers.
13. Sarkar, P. and J. Rajtar. *Transient well testing of coalbed methane reservoirs with horizontal wells*. in *Permian basin oil and gas recovery conference*. 1994. Society of Petroleum Engineers.
14. Clarkson, C.R., et al. *Production data analysis of fractured and horizontal CBM wells*. in *SPE eastern regional meeting*. 2009. Society of Petroleum Engineers.
15. Nie, R.-S., et al., *Modeling transient flow behavior of a horizontal well in a coal seam.* International Journal of Coal Geology, 2012. **92**: p. 54-68.
16. Jiang, R., et al., *Production Performance Analysis for Multi-Branched Horizontal Wells in Composite Coal Bed Methane Reservoir Considering Stress Sensitivity.* Journal of Energy Resources Technology, 2020. **142**(7).

17. Wei, Z., et al., *Production performance analysis for horizontal wells in composite coal bed methane reservoir.* Energy Exploration & Exploitation, 2017. **35**(2): p. 194-217.
18. Pedrosa, O. *Pressure transient response in stress-sensitive formation*. in *Paper SPE15115, presented at the 1986 SPE California regional meeting. Oakland, April*. 1986.
19. Langmuir, I., *The constitution and fundamental properties of solids and liquids. Part I. Solids.* Journal of the American chemical society, 1916. **38**(11): p. 2221-2295.
20. Van Everdingen, A. and W. Hurst, *The application of the Laplace transformation to flow problems in reservoirs.* Journal of Petroleum Technology, 1949. **1**(12): p. 305-324.
21. Stehfest, H., *Algorithm 368: Numerical inversion of Laplace transforms [D5].* Communications of the ACM, 1970. **13**(1): p. 47-49.
22. Ozkan, E. *New solutions for well-test-analysis problems: part III-additional algorithms*. in *SPE Annual Technical Conference and Exhibition*. 1994. Society of Petroleum Engineers.